J Mater Sci (2008) 43:64–74
DOI 10.1007/s10853-007-2094-8

Effect of compatibilization on mechanical and thermal properties of polypropylene–soy flour composites

R. R. N. Sailaja · B. G. Girija · Giridhar Madras · N. Balasubramanian

Received: 13 April 2007 / Accepted: 10 August 2007 / Published online: 26 September 2007

Abstract A new biobased composite was developed by adding soy flour (SF) to polypropylene (PP). This composite shows an enhanced tensile strength and modulus but decrease in elongation at break. The compatibilizer (coupling agent) appears to have a synergistic effect on tensile strength. The presence of the compatibilizer improves the dispersion of SF in the PP matrix. The addition of glycerol plasticizer to the composite improves the processability resulting in improved performance, as compared to composites without glycerol plasticizer. The optimal compatibilizer content appears to be 6%.

Introduction

The development of biobased plastics has been of considerable interest for the past three decades. The development of these plastics has been triggered by the emphasis on solid waste management and environmental concerns. Polyolefins, especially polyethylene and polypropylene (PP), are used extensively for various applications. However, post-consumption disposal of these materials has posed a serious threat to the environment owing to their non-degradability. Bacterial polyesters like polyhydroxy alkaonates are possible alternatives to polyolefins but their high cost limits their use. Therefore, a possible solution is to blend synthetic polymers with renewable materials from the agricultural feedstocks.

Soy flour (SF) is an inexpensive, abundantly available, and renewable resource, which can be incorporated as a potential biobased component in polyolefins like polypropylene. Soy-based plastics have been in vogue for quite sometime to represent the family of green plastics [1]. However, owing to their inferior mechanical properties, they have not been commercialized. There have been a few studies [2–5] to improve the mechanical properties of soy plastics by reinforcement with cellulose powder, Indian grass fiber, and pineapple leaf fiber. These reinforcements improved the mechanical properties to an extent, which was further enhanced by adding a compatibilizer. It was observed that, although, the tensile and flexural strength increased, there was no improvement in impact strength [6–8]. The use of green composites including the soy-based plastics has been summarized in a review [9]. The addition of a compatibilizer has been observed to improve the interfacial adhesion between the biopolymer and the synthetic polymer [10]. Addition of toluene diisocyanate compatibilizer to a blend of soy protein with polycaprolactone resulted in improved water resistance and tensile strength [11]. Similar improvements in tensile properties were observed when glutaraldehyde was added as a compatibilizer [12].

The modification of SF by adding a plasticizer or a crosslinker has been found to be beneficial. Thus, crosslinkers such as formaldehyde, ethylene glycol diglycidyl ether, glyoxal [13–15],or plasticizers like glycerol and acetamide exhibited better mechanical properties than their unmodified counterparts [16, 17]. It was shown [18] that

R. R. N. Sailaja (✉)
The Energy and Resources Institute (TERI), Southern Regional Centre, Bangalore 560071, India
e-mail: rrnsb19@rediffmail.com

B. G. Girija · G. Madras
Department of Chemical Engineering, Indian Institute of Science, Bangalore 560012, India

N. Balasubramanian
R.V. College of Engineering, Bangalore 560059, India

soy protein modified by thiosemicarbazide could be used for developing molded products.

Soy flour is cost effective and is comparable with other forms of soy protein [4]. However, to the best of our knowledge, no studies have been reported on the blends of SF with polypropylene. In this study, we have developed two blends, namely soy flour-PP (SF-PP) and plasticized (by glycerol) soy flour-PP (PSF-PP) and investigated its mechanical, thermal, and ageing properties In addition, we have also examined the use of a compatibilizer in these composites and investigated the properties of this material.

Experimental

Synthesis of compatibilizer and PSF

Polypropylene (24FS040) with melt flow index of 10 g $(10\ min)^{-1}$ from Reliance Petrochemicals was used. Soy flour was obtained locally. Maleic anhydride-grafted polypropylene (MAPP) was synthesized [19] by grafting maleic anhydride and benzoyl peroxide as initiator onto polypropylene by solution polymerization in xylene at 120 °C. The grafted product was subjected to Soxhlet extraction for 15 h to remove the unreacted maleic anhydride. The grafting percentage, as suggested by Gaylord and Mehta [19], was 1.2%. The FTIR spectra in Fig. 1 shows the characteristic –C=O– bond at 1710 cm^{-1}. Plasticized soy flour (PSF) was prepared by mixing 48% of SF with 33% glycerol and 19% distilled water for 1 h and then heated at 70 °C in a constant temperature water bath. The resulting PSF was stored in polyethylene bags in the refrigerator.

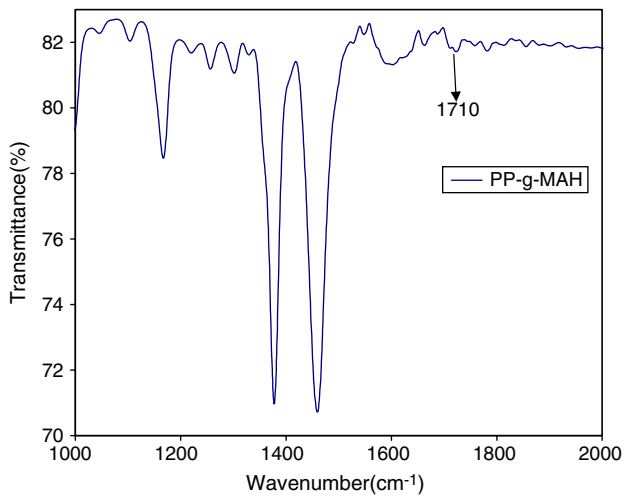

Fig. 1 FTIR spectra for PP-g-MAH

Blend preparation

Two types of blends were prepared, namely, PP-SF and PP-PSF. The blend components were prepared by melt mixing at 210 °C in a locally fabricated kinetic mixer where small quantities can be used. Dumbbells-shaped specimens were then molded as per ASTM specifications into standard dies supplied with the Mimimax molder (Custom Scientific Instruments, New Jersey, USA, Model CS-183MMX). The amount of compatibilizer added is expressed as the weight percent of SF. These dumbbell specimens were then subjected to impact and tensile tests using Minimax testing units.

Mechanical properties of the blend

A Minimax impact (Model CS-183T1079) and tensile tester (model CS-183TTE) (custom Scientific Instruments, NJ, USA) was used to measure (unnotched) impact strength and tensile properties, respectively. At least eight specimens were tested for each variation in the composition of the blend. The impact and tensile tests were performed as per ASTM D1822 and ASTM D1708 methods, respectively. The strain rate used for all tensile measurements is 10 mm/min.

Thermal analysis

Thermogravimetric analysis (TGA) was carried out for the SF as well as for the blends using Perkin-Elmer Pyris Diamond 6000 analyzer in nitrogen atmosphere. The sample was subjected to a heating rate of 10 °C/min in the heating range of 40–600 °C using Al_2O_3 as the reference material. Differential Scanning Calorimetry (DSC) of the blend specimens was performed in a Mettler Toledo DSC 822e model. Samples were placed in sealed aluminum cells using a quantity less than 10 mg and scanned at a heating rate of 10 °C/min from 25 to 200 °C.

Blend morphology

Scanning electron microscope (SEM) (JEOL, JSM-840 a microscope) was used to study the morphology of fractured and unfractured specimens. The specimens were gold sputtered prior to microcopy (JEOL, SM-1100E). The morphology of the unfractured blend specimens was taken after soaking the samples for 48 h in water at 80 °C.

Results and discussion

Soy flour has been incorporated as biobased filler in PP/SF composites. In order to improve the processability of the

blend, glycerol has been added as a plasticizer to these blends.

Relative impact strength (RIS)

Figure 2 shows that impact strength vs. compatibilizer percentage for PP/SF and PP/PSF blends. PP/PSF blends exhibit better impact strength than the PP/SF blends although in both cases, the impact strength reduces as SF/PSF loading increases. The impact strength (energy absorbed per unit area of cross section) of pure PP is 1.2×10^2 kJ/m^2. For PP/PSF blends, the impact strength is nearly 80% of neat PP on adding 9% of MAPP compatibilizer. However, compatibilized PP/SF blends attain only 70% (of PP) impact strength values with 40% SF loading. For higher i.e., 50% SF content, there is no significant improvement even after adding MAPP. For PP/SF blends, the impact strength attains an optimal value with 6% compatibilizer.

Stress–strain behavior

Figure 3(a) and (b) shows the engineering stress–strain curves for PP/SF and PP/PSF blends, respectively. The stress–strain curve for pure PP (curve (a)) is also given in the figures for the sake of comparison. In Fig. 3(a), the addition of 20% SF (curve (b)) drastically reduces stress and strain and the blend exhibits the typical brittle behavior. Addition of compatibilizer to this blend does not improve the ductility (curve (c)) but the ultimate strength is almost at par with that of neat PP. For higher SF loading of 40% the uncompatibilized blend (curve (d)) exhibits brittleness while its compatibilized counterpart (curve (e)) is even more brittle but shows an improvement in ultimate strength. In Fig. 3(b), the uncompatibilized blend with 20% PSF loading (curve (b)) shows a drastic reduction in strain although there is no significant reduction in strength. The compatibilized blend shown in curve (c) shows considerable improvement in elongation. In most of the polymer/filler systems there is usually a trade off between improvements in ductility or ultimate strength on compatibilization. In this case too, the ductility does not improve on compatibilization. However, an increase in PSF loading to 40% shows a reverse behavior. The uncompatibilized blend (curve (d)) has lower strength and better ductility than compatibilized blend (curve (e)), which is characterized by higher strength and slightly lowered ductility. Soy flour consists of polar and non-polar side chains. This leads to hydrogen bonding, dipole–dipole interactions that restrict the mobility of the chain segments. Addition of glycerol plasticizer eases these intra and intermolecular interactions, thereby improving the processability of the PP/PSF blends.

Relative tensile strength

Figure 4(a) and (b) shows the variation of the relative tensile strength (RTS) vs. percent compatibilizer for different SF and PSF loadings (tensile strength of pure PP is 23 MPa). Addition of SF/PSF to PP did not significantly affect the tensile strength of PP up to 40% loading. For 50% SF/PSF loading, the tensile strength slightly reduced but on adding MAPP compatibilizer, the tensile strength is 90% (of PP) in PP/SF blends and 97% (of PP) in PP/PSF blends. Soy flour contains amine and hydroxyl groups which are compatible with the carboxyl group of maleic anhydride, i.e., MAPP. The possible reaction scheme is given in Fig. 4(c). However, on adding compatibilizer, the tensile strength values do not significantly exceed that of

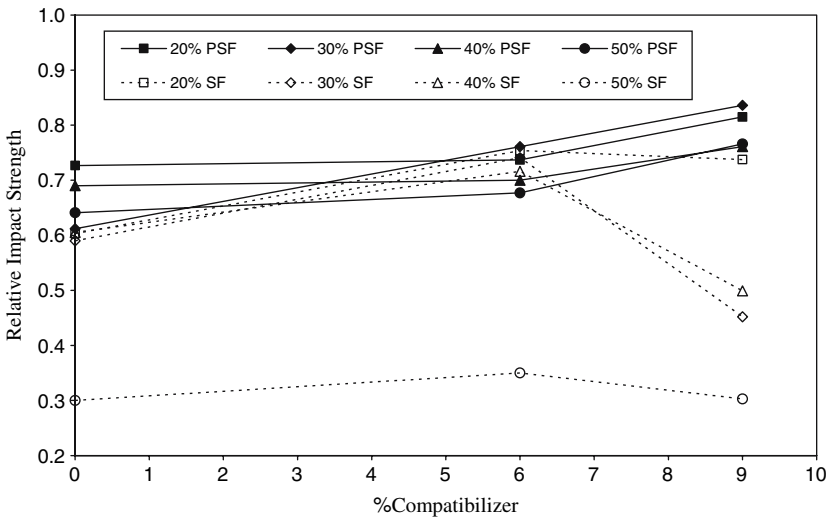

Fig. 2 Relative impact strength vs. percentage compatibilizer for the PP/SF and PP/PSF composites

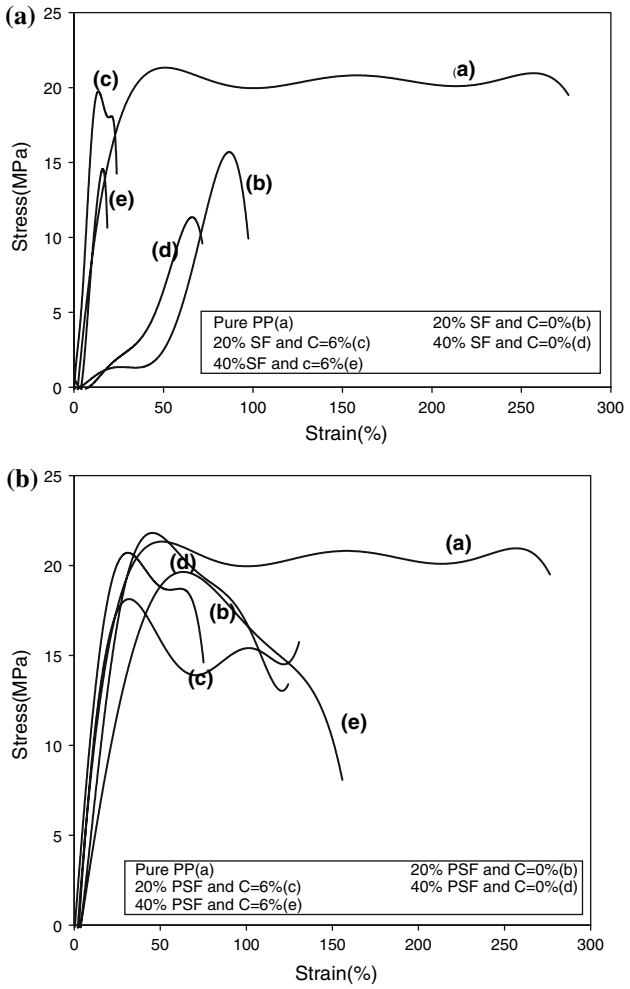

Fig. 3 Stress–strain curves for (**a**) PP/SF (**b**) PP/PSF composites

pure PP. The other biobased fillers used in our previous study i.e. starch, wood pulp, and lignin [9–11] showed drastic reduction in tensile strength with increasing filler content which is not so in the case of SF. This suggests that high loadings of SF/PSF are possible without affecting the tensile strength and at the same time impart biodegradability to PP. The tensile strength values for PP/PSF blends were higher than PP/SF blends.

Figure 5 shows SEM micrographs for the fractured section of the specimens. Figure 5(a) and (b) shows the fracture section morphology for uncompatibilized and compatibilized blends with 20% PSF loading. Figure 5(a) shows extensive cavitation and crazing while Fig. 5(b) exhibits extensive shearing with short fibrils accompanied by cavitation of SF particles. Extensive shearing with large holes due to debonding of SF is observed for uncompatibilized blend with 50% PSF loadings (Fig. 5c). Shearing and cavitation absorb large amount of energy thereby leading to high tensile strength of the material. The compatibilized counterpart shown in Fig. 5(d) shows shearing and comparatively smaller holes left by SF owing to better dispersion of SF facilitated by compatibilizer with addition of MAPP. For PP/SF blend with 20% SF loadings, the SEM micrograph (Fig. 5e) shows brittle fracture and larger holes. The compatibilized blend exhibits a quasi-brittle fracture characterized by short fibrils and smaller holes left by cavitations of SF (Fig. 5f). The PP/PSF blends show more ductility than PP/SF blends and this thereby, leads to better mechanical properties. Glycerol as plasticizers imparts flexibility and thermoplasticity to SF and thereby eases the processability of the blend.

Relative tensile modulus

The plots of relative tensile modulus (RYM) vs. compatibilizer percentage for PP/SF and PP/PSF blends are shown in Fig. 6(a) and(b), respectively (tensile modulus of pure PP is 0.27 GPa). For PP/SF blends (Fig. 6a), the tensile modulus increases as SF loading increases due to rigidity of SF chains. Compatibilization with MAPP reduces the modulus values due to interface effects. A similar trend is also observed for PP/PSF blends as shown in Fig. 6(b).

Relative elongation at break

Figure 7(a) and (b) shows a plot of relative elongation at break (REB) vs. compatibilizer percentage for PP/SF and PP/PSF blends respectively (elongation at break for neat PP is 300%). PP/SF and PP/PSF blends, the REB values are reduced drastically as SF loading increases. Addition of compatbilizer marginally improves the elongation at break values. The REB values for PP/PSF blends were higher than PP/SF. For 20% PSF loading, the REB values increased for 0.43 to 0.74, i.e., 74% of that of pure PP as shown in Fig 7(b). For higher PSF loadings there is no significant improvement in elongation at break.

Blend morphology (surface section)

Figure 8 shows the blend surface section morphology of PP/PSF blends. The SEM micrograph of uncompatibilized PP/PSF blend with 20% PSF loading is shown in Fig 8(a). This is characterized by larger holes and plane surface. The compatibilized specimens (Fig. 8b) shows a coarser surface owing to compatibilization. This feature is more prominent for higher, i.e., 40% PSF loading as shown in Fig. 8(c). The larger holes left by agglomerated PSF particles owing to lack of compatibility between hydrophilic polar PSF and hydrophobic non-polar PP. The compatibilized specimen counterpart shown in Fig. 8(d) shows

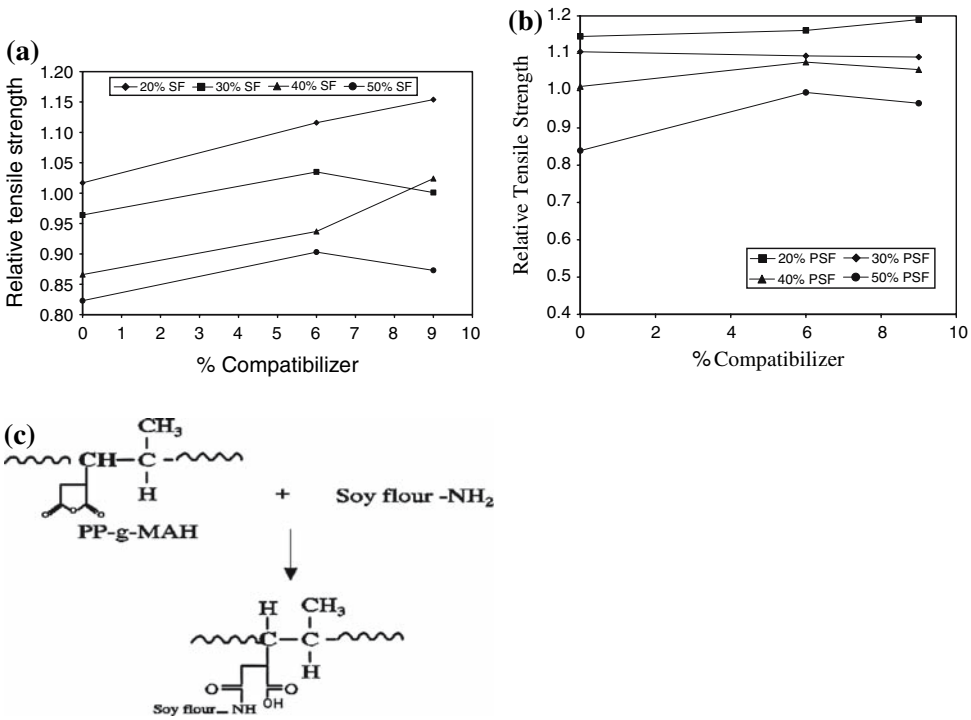

Fig. 4 Relative tensile strength vs. percentage compatibilizer for (**a**) PP/SF and (**b**) PP/PSF composites. (**c**) Possible reaction mechanism between SF and functionalized PP

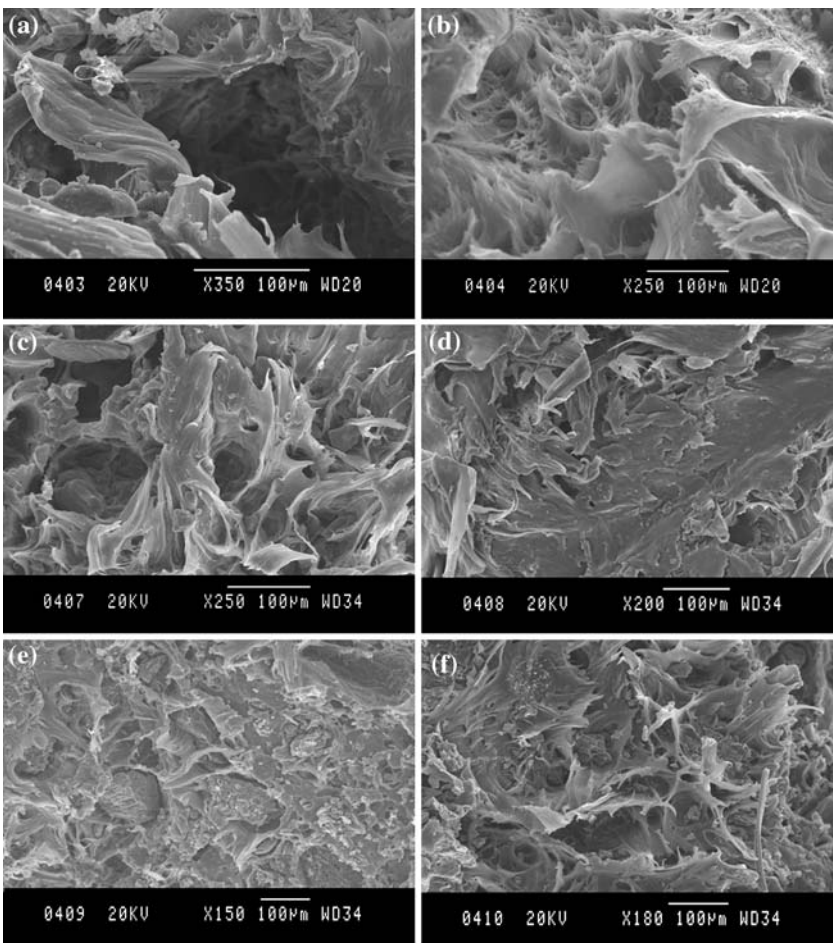

Fig. 5 SEM photographs of the fracture section for various blends (**a**) 20% PSF and C = 0% (no compatibilizer), (**b**) 20% PSF and C = 6%, (**c**) 50% PSF and C = 0% (no compatibilizer), (**d**) 50% PSF and C = 6 %, (**e**) 20% SF and C = 0%, and (**f**) 20% SF and C = 6%

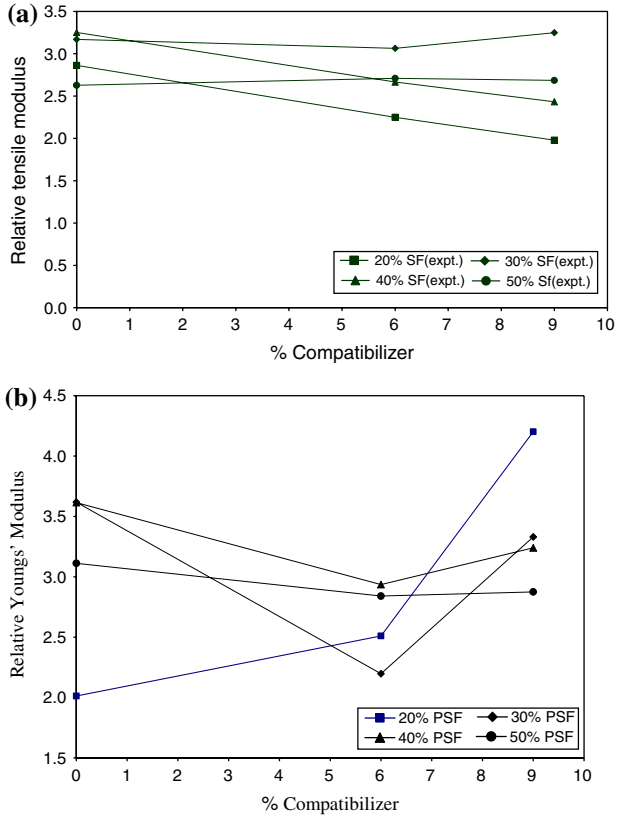

Fig. 6 Relative tensile modulus for (**a**) PP/SF and (**b**) PP/PSF composites

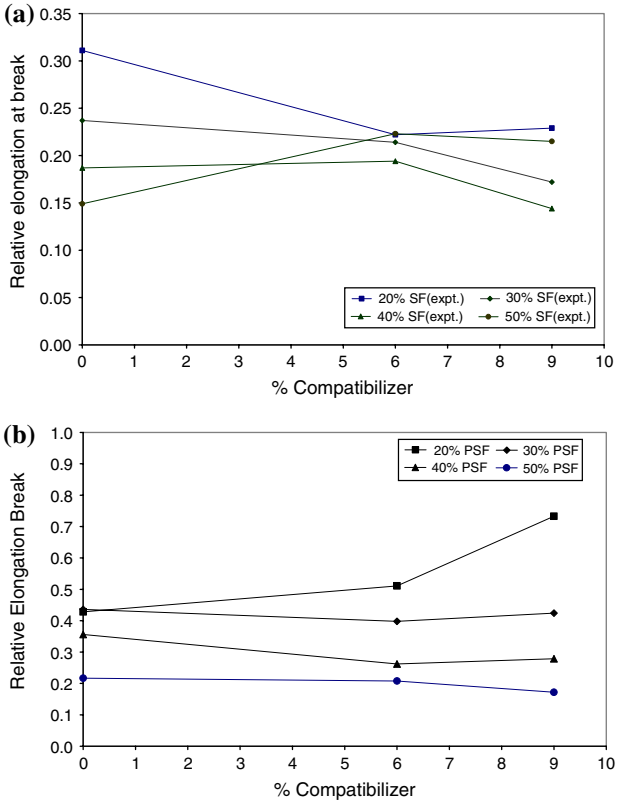

Fig. 7 Relative elongation at break for (**a**) PP/SF and (**b**) PP/PSF composites

smaller holes indicating good dispersion. A similar observation is seen in Fig. 8(e) and (f) for PP/SF blends. The uncompatibilized composite specimen shows holes due to removal of SF particles in Fig. 8(e). The compatibilized specimen on the other hand shows an interlocked surface indicating some resistance to the removal of SF from the blend (Fig. 8f).

Effect of SF content

Figure 9(a–c) shows the effect of SF/PSF content on the mechanical properties of SF/PP and PSF/PP composites. Figure 9(a) shows the RTS value vs. SF or PSF loading from 20% to 50%. However, PSF/PP composites exhibit higher impact strength values than SF/PP blends. The compatibilized SF/PP and PSF/PP blends exhibit higher RTS values with 6% and 9% compatibilizer, respectively. A similar trend is observed for relative tensile strength values as shown in Fig. 9(d). It is interesting to note that a loading of 50% SF or PSF to PP does not drastically affect the tensile strength of these composites, although compatibilization improves the tensile strength to values slightly higher than neat PP. Three mathematical models have been used to predict tensile strength for PP/SF blends. One of them is the Nicolais and Narkis model [20]

$$RTS = \frac{\sigma_b}{\sigma_{PP}} = 1 - 1.21\phi_f^{2/3} \tag{1}$$

In the above equation σ_b and σ_{PP} are the tensile strength values for blend and neat PP, respectively. ϕ_f is the volume fraction of SF. The volume fractions have been calculated as suggested by Willett [20] given in equation below

$$\phi_i = \frac{W_i/\rho_i}{\sum W_i/\rho_i} \tag{2}$$

In the above equation ρ_i and W_i are the density and weight fraction of component i in the blend. The density values of PP have been taken to be 0.97 g/cm^3 and that of SF has been measured to be 1.21 g/cm^3, respectively. The calculated values from Eq. 2 are much lower than experimental values (not shown). This model assumes no interaction between matrix and filler. Hence, it is not surprising that this model does not explain our results. This is due to the use of compatibilizer to promote interaction between the filler and matrix. Further, there may be mechanical bonding due to the amorphous dispersed phase being compressed by the matrix crystalline phase [21].

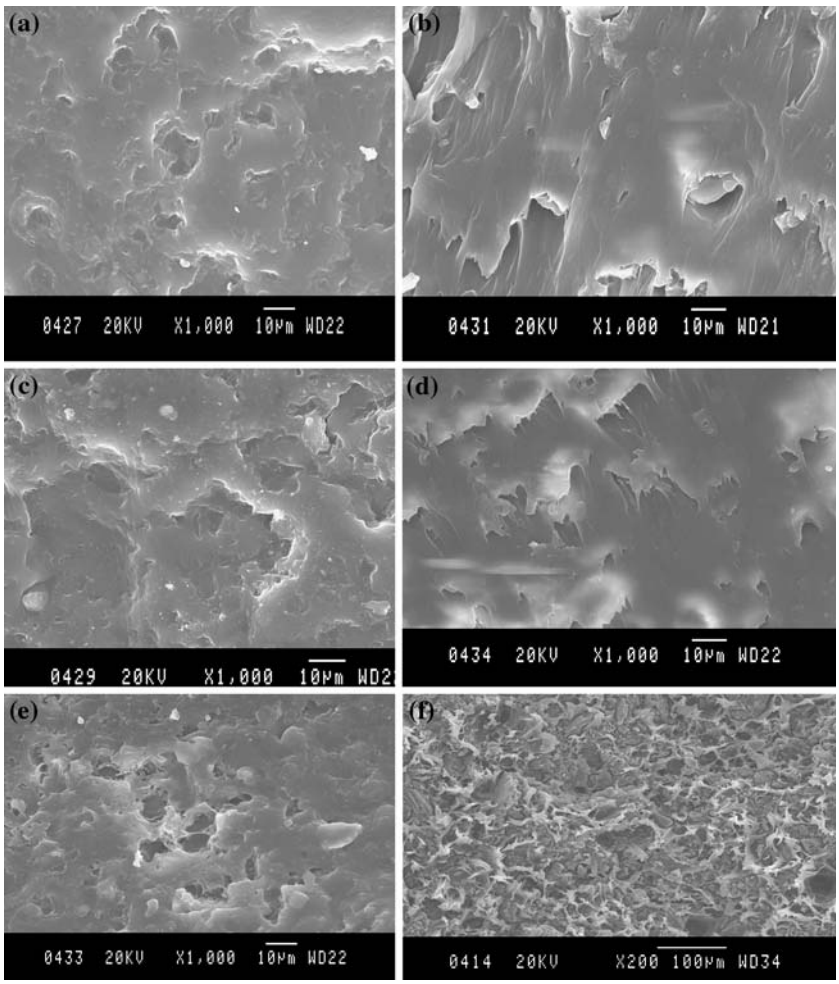

Fig. 8 SEM photographs for blend morphology (surface section): (**a**) 20% PSF loading and C = 0% (no compatibilizer), (**b**) 20% PSF loading and C = 6%, (**c**) 40% PSF and C = 0% (no compatibilizer), (**d**) 40% PSF and C = 6%, (**e**) 40% SF and C = 0%, and (**f**) 40% SF and C = 6%

The second model [22] is adapted from Halpin–Tsai equation for modulus and is given by

$$RTS = \frac{\sigma_b}{\sigma_{PP}} = \frac{1 + G\eta_T\phi_f}{1 - \eta_T\phi_f} \tag{3}$$

where η_T is given by,

$$\eta_T = \frac{R_T - 1}{R_T + G} \tag{4}$$

where R_T is the ratio of filler tensile strength to tensile strength of PP (unfilled). G is constant given in Eq. 5 below

$$G = \frac{7 - 5\upsilon}{8 - 10\upsilon} \tag{5}$$

In Eq. 5, υ is the Poisson's ratio of PP and is taken to be 0.35. The R_T values calculated to match the experimental data has been found to be 0.9. Figure 9(a) shows the theoretical values obtained from Eq. 2. It can be seen from Fig. 9(a) that the theoretical values are close to the experimental values indicating good interactions between the blend compounds.

The model of Turcsanyi [22] discusses the composition dependence using the following empirical equation:

$$RTS = \frac{1 - \phi_f}{1 + 2.5\,\phi_f}\exp(B\phi_f) \tag{6}$$

In the above equation the parameter B, depends on interfacial properties. B was determined to match the experimental results by trial and error. B was found to be 2.9, which suggests improved adhesion [22].

It is interesting to note that both modified Halpin–Tsai and Turcsanyi model predictions are close to each other. The observed experimental results are also in the close vicinity of the predicted results indicating good adhesion between the matrix and filler. Further, the tensile strength values of PSF-PP blends are above the theoretical line while in the case of SF-PP blends, the values are lower than the theoretical values for SF loadings beyond.

The tensile modulus for SF/PP and PSF/PP blends increases as SF or PSF content increases (Fig. 9(b)). Addition of 6% and 9% compatibilizer improves the dispersion of SF or PSF in PP. This increase in modulus may

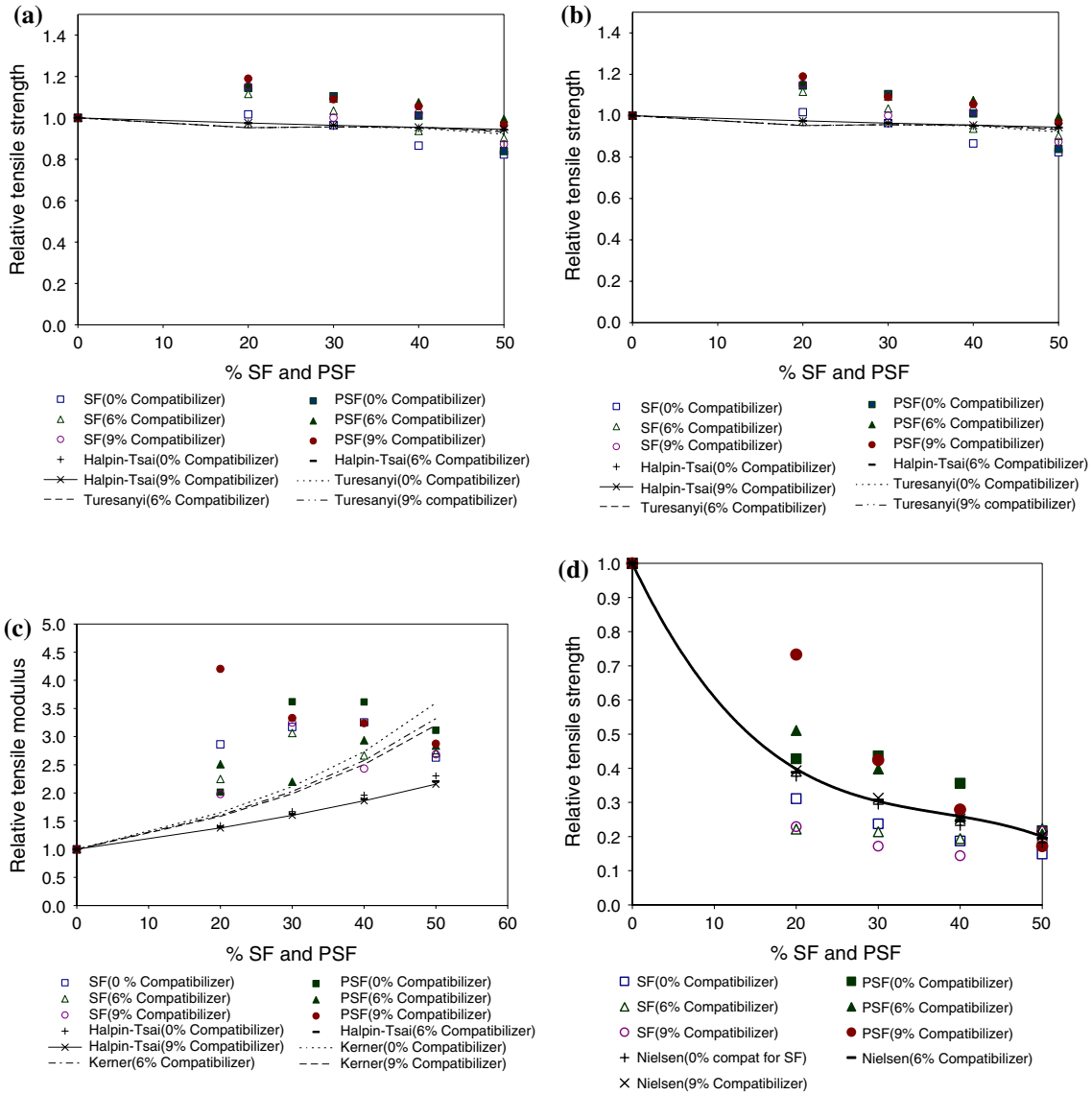

Fig. 9 The variation of the (**a**) Relative impact strength, (**b**) Relative tensile strength, (**c**) Relative tensile modulus, and (**d**) Relative elongation at break with SF or PSF content

be due to the rigidity in sugar and protein chains in SF. A comparison is made between two models for the prediction of modulus for PP/SF blends. One of them is the Kerner's model [20],

$$RYM = \frac{E_b}{E_{PP}} = \left[1 + \left(\frac{\phi_f}{1-\phi_f}\right)\left(\frac{15(1-\upsilon)}{(8-10\upsilon)}\right)\right] \tag{7}$$

In the above equation, E_b and E_{PP} are the tensile modulus values for the blend and pure PP, respectively. The experimental data does not match with the theoretical data as shown in Fig. 9(b). In this model poor bonding between the filler and matrix is assumed. This suggests that some adhesion exists between SF and PP.

The other model is the modified Halpin–Tsai model for RYM given in Eq. 8 below [20],

$$RYM = \frac{E_b}{E_{PP}} = \left[\frac{1+G\eta_m\phi_f}{1-\eta_m\phi_f}\right] \tag{8}$$

where

$$\eta_m = \frac{R_m - 1}{R_m + G} \tag{9}$$

where G is same as in Eq. 6, R_m is the ratio of filler modulus to matrix modulus, i.e., modulus of PP. The R_m value has been found by trial and error to match the experimental results that has been found to be 6. The

experimental values are higher than what the model predicts and obtained values are probably due to interfacial effects.

SF or PSF loading has a drastic effect on REB as observed in Fig. 9(c). The REB values reduce to less than 0.2 (i.e., 20% of neat PP). Further, compatibilization marginally improves elongation at break.

The Nielsen's model [20] for perfect adhesion calculates the REB values as per Eq. 10 below

$$REB = \frac{\varepsilon_b}{\varepsilon_{PP}} = \left(1 - k\,\phi_f^{1/3}\right) \tag{10}$$

where ε_b and ε_{PP} are elongation at break values for the blend and neat PP, respectively. In Eq. 10, k is an adjustable parameter, which depends on filler geometry. The k value has been found to be 0.98. The experimental values are lower than predicted values, which suggest that the adhesion between filler and matrix is weak as perfect adhesion in heterogeneous blends is not possible as shown in Fig. 9(c).

Thermal ageing

The samples were soaked in 1(N) NaOH solution at 70 °C for 8 days and the weight loss percentage for compatibilized and uncompatibilized specimens has been evaluated as shown in Fig. 10(a) and (b) for PP/SF and PP/PSF composites, respectively. In Fig. 10(a), the compatibilized blends showed a slightly higher weight loss percentage as compared to uncompatibilized blends. However, in either case, the % weight loss increases as SF content increases.

The PP/PSF blends show a higher weight loss than PP/SF blends as shown in Fig. 10(b) although the trend is similar to Fig. 10(a).

Thermogravimetric analysis

Figure 11(a) shows the TGA/DTG curves for PP/SF blends. Pure SF (curve (a)) undergoes thermal decomposition at 312 °C in a single stage with a large amount of

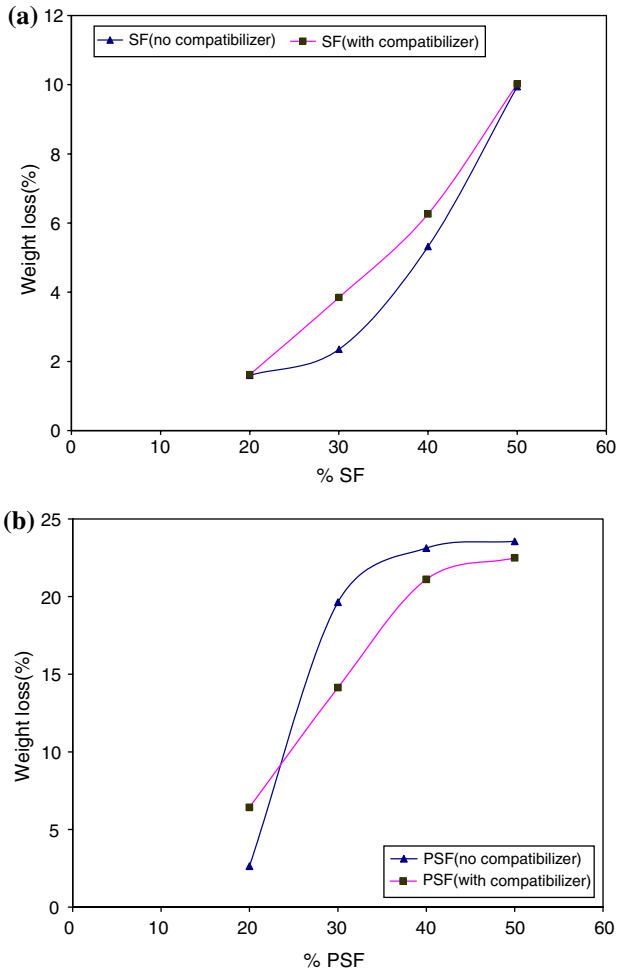

Fig. 10 Thermal ageing for (**a**) PP/SF and (**b**) PP/PSF composites

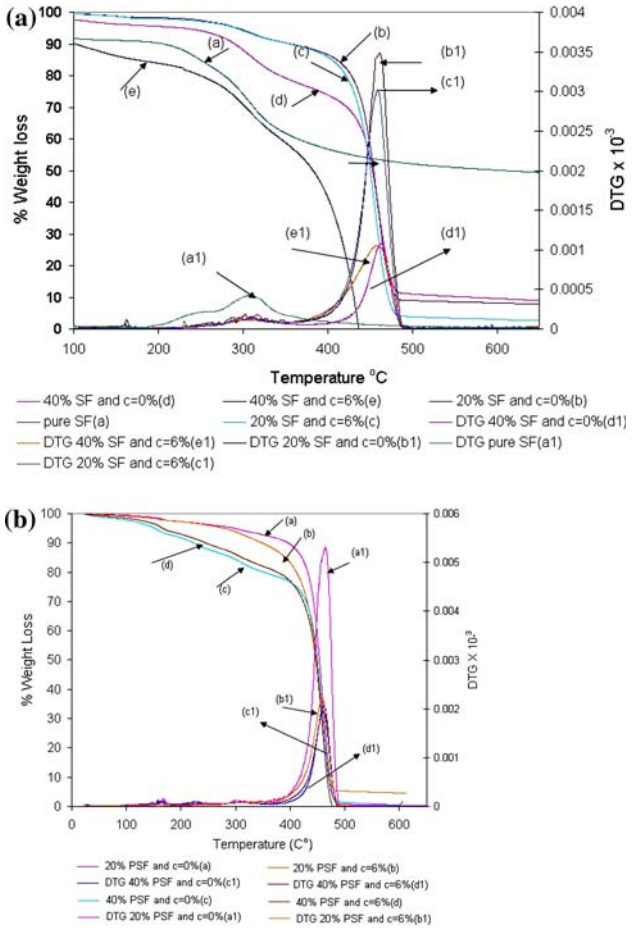

Fig. 11 TGA/DTG Thermograms for (**a**) PP/SF and (**b**) PP/PSF composites (C = 0% denotes that no compatibilizer has been added to the blend)

char content [23]. For 20% SF loading (no compatibilizer), the TGA curves shows a two-stage (curve (b)) degradation with a, broad peak at 313 °C for SF due to the cleavage of glucoside units while breakage of –C–C– backbone takes place at 463 °C. The compatibilized counterpart shown in curve (c) shows a slight lowering of degradation temperatures accompanied by higher weight loss indicating better interaction between the blend components. The effect of compatibilizer is more pronounced at higher SF loading, i.e., 40% as shown in curves (d) and (e). The uncompatibilized blend (curve (d)) shows two-stage degradation with final char content of 30%. The compatibilized blend (curve (e)) shows only 2% char content.

Figure 11(b) shows the TGA/DTG curves for PSF/PP blends. All the blends (curves (a) to (e)) show a three-stage degradation. The first stage around 155 °C is due to the decomposition of glycerol plasticizer. The second stage at 310 °C due to decomposition of SF while the third stage at 460 °C is attributed to PP degradation. The trend is similar to SF/PP blends.

Activation energy

Thermo gravimetric analysis data (TGA) is used to determine the kinetic parameters of the pure sample and blends. The reaction mechanism is assessed by the activation energy of the decomposition of blends and pure sample. The rate equation [24, 25], expresses the rate of conversion at a constant temperature as a function of the loss of reactant concentration and rate coefficient

$$\ln\left(\frac{dx}{dt}\right) = \ln A + n\ln(1-x) - \frac{E_a}{RT} \tag{11}$$

where x is fractional conversion, A is the frequency factor and E_a is the activation energy. The parameter R, T, and n represent the universal gas constant, temperature in K, and the order of reaction, respectively. Friedman's analysis based on Eq. 11 suggests that the activation energy can be directly obtained from the slope of linearly regressed line of $\ln(dx/dt)$ vs. $1/T$. According to Kissinger method [26], which is also recommended by ASTM [27], the activation energy is obtained from the slope of linearly regressed line of $\ln(\beta/T_p^2)$ vs. inverse of T_p where T_p represents the peak of decomposition temperature and β represents the heating rate.

The above two methods were used to calculate the activation energies of degradation. The activation energy obtained by Friedman's technique by plotting $\ln(dx/dt)$ vs. $1/T$ is 77 kJ/mol (Fig. 12(a)) and it is comparable to the activation energy of 78 kJ/mol by Kissinger method (Fig. 12(d)).

Figure 12(a) shows linearly regressed lines corresponding to dynamic experiments carried out at different heating rates: 5, 10, 15, 20, 25 °C/min for SF. These decomposition processes are a single-stage decomposition reaction. The degradation temperature rises with increasing of the heating rate. The activation energy values for blends

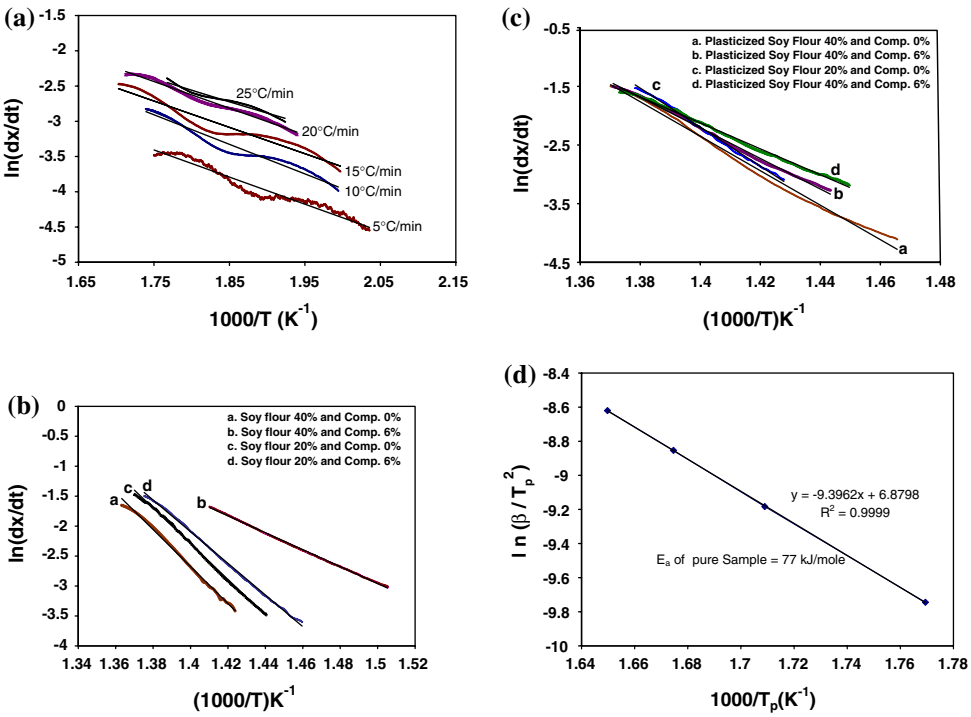

Fig. 12 (**a**) Differential weight loss vs. reciprocal temperature (Friedman's) at varying heating rates to determine the activation energy of SF, (**b**) Activation energy for SF obtained by Friedman's method, (**c**) Activation energy for PSF obtained by Friedman's method, and (**d**) Activation energy by Kissinger's method based on peak temperature and heating rate to determine the activation energy of SF

Table 1 Activation energies of the blends and pure sample

Composition	E_a of pure sample (kJ/mol)	E_a without compatibilizer (kJ/mol)	E_a with (6%) compatibilizer (kJ/mol)
Pure Soy flour	77		
PP-40% SF		256	117
PP-20% SF		247	219
PP-40% PSF		235	216
PP-20% PSF		275	183
PP	285		

Data on PP from Saitoh and Nishizaki, quoted in [28].

obtained are shown in Table 1. It shows that there is significant change in the activation energy values between pure sample and uncompatibilized blends (Fig. 12(b)) and compatibilized blends (Fig 12(c)), whereas the blends without compatibilizer shows higher values than the pure samples and plasticized or with compatibilizer blends. This indicates that the compatibilized blends need lower energy and are less thermally stable compared to uncompatibilized blends but more stable than the pure samples. The addition of SF reduces the activation energy of the blends, which further decrease on compatibilization owing to better interfacial interactions between the two phases.

Conclusions

A biobased composite of polypropylene with SF was developed. The use of biobased material is expected to promote biodegradability. These composites (containing up to 50% SF) have been characterized for various mechanical and thermal degradation properties. Models were used to determine the various parameters from the experimental data. The effect of plasticizer and compatibilizer was also examined. The use of glycerol as plasticizer improves the processability of the composite and the impact, tensile strength, modulus, and elongation at break. The use of maleic anhydride as a compatibilizer improved modulus of the composite but decreased the tensile and impact strength and ductility. An attempt was made to optimize the mechanical properties by a combination of PSF and compatibilizer content. For instance, composites containing up to 40% PSF and 6% compatibilizer have a tensile strength nearly equal to that of PP but has a higher modulus than PP and a 25% reduced impact strength. To retain ductility at 75% of PP level, PSF must be restricted to 20% and compatibilizer used to 9% of PSF content. The thermal degradation studies indicate that the addition of SF reduces the activation energy of the blends and these activation energies are further reduced for compatibilized composites.

Acknowledgements We thank Dr. V Prakash, Central Food Technology Research Institute for the sample of soy flour used in this work. NB is grateful to All India Council of Technical Education for the award of Emeritus Fellowship.

References

1. Sue H-J, Wang S, Jane JL (1997) Polymer 38:5035
2. Liu W, Mohanty AK, Askeland P, Drzal LT, Misra M (2004) Polymer 45:7589
3. Paetau I, Chen C, Jane J (1994) Ind Eng Chem Res 33:1821
4. Tummala P, Mohanty AK, Misra M, Drzal LT, Presented at American Society of Composites 2002 Annual Meeting (17th Annual Technical Conference), 21–23 October 2002, West Lafayette, Indiana
5. Liu W, Misra M, Askeland P, Drzal LT, Mohanty AK (2005) Polymer 46:2710
6. Zhang Z, Sun SX (2003) J Appl Polym Sci 88:407
7. Huang J, Zhang L, Wang X (2003) J Appl Polym Sci 89:1685
8. Liu W, Mohanty AK, Drzal LT, Misra M (2005) Ind Eng Chem Res 44:7105
9. Mohanty AK, Misra M, Drzal LT (2005) J Polym Environ 10:19
10. Graiver D, Waikul LH, Berger C, Narayan R (2004) J Appl Polym Sci 92:3231
11. Deng R, Chen Y, Chen P, Chang L, Liw B (2006) Polym Degrad Stabil 91:2189
12. Chen P, Zhang L, Gu J (2006) J Appl Polym Sci 101:334
13. Wang N, Zhang L, Gu J (2004) J Appl Polym Sci 95:465
14. Swain SN, Rao KK, Nayak PL (2005) Polym Int 54:739
15. Vaz CM, Van Doeveren PFNM, Yilmaz G, DeGraf LA, Reis RL, Cunhan AM (2005) J Appl Polym Sci 97:604
16. Liu D, Zhang L (2006) Macromol Mater Eng 291:820
17. Guang-Heng W, An-Wing Z, Xiao-Bing H (2006) J Appl Polym Sci 102:3135
18. Nanda PK, Rao KK, Nayak PL (2007) J Appl Polym Sci 103:3134
19. Gaylord NG, Mehta R (1988) J Polym Sci Part A: Polym Chem A26:1188
20. Willett JL (1994) J Appl Polym Sci 54:1685
21. Rodriguez-Gonzalez FJ, Ramsay BA, Favis BD (2003) Polymer 44:1517
22. Bliznakov ED, White CC, Shaw MT (2000) J Appl Polym Sci 77:3220
23. Chabba S, Mathews GF, Netravali AN (2005) Green Chem 7:576
24. Girija BG, Sailaja RRN, Madras G (2005) Polym Degrad Stabil 90:147
25. Friedman HL (1965) J Polym Sci 50:183
26. Kissinger HE (1957) Anal Chem 29:1702
27. ASTM E 698–79 (1979) Appendix X3, American Society of Testing Materials, Philadelphia, PA, USA
28. Dickens B (1982) J Polym Chem Edu 20:1169